Contrib Mineral Petrol (2017) 172:8
DOI 10.1007/s00410-016-1327-8

ORIGINAL PAPER

Effect of pressure on closure temperature of a trace element in cooling petrological systems

Yan Liang[1]

Received: 25 August 2016 / Accepted: 22 December 2016 / Published online: 25 January 2017

Abstract Closure temperature is important to many diffusion-related problems involving cooling. The classic model of Dodson and its modifications for cooling petrological systems are formulated at constant pressure. Many petrologic processes involve changes in both temperature and pressure. The effect of changing pressure on diffusional loss in cooling petrological systems has not been considered in Dodson's model. During upwelling, the decompression rate is related to the cooling rate through the slope of the upwelling path. Simple analytical expressions for the average or mean closure temperature and closure pressure in cooling-upwelling mono-mineralic and bi-mineralic systems are obtained by noting that both temperature and pressure decrease as a function of time along the upwelling path. These pressure-adjusted equations are nearly identical to closure temperature equations for isobaric cases if one replaces the activation energy and pre-exponential factor for diffusion in the isobaric formulations by the path-dependent activation energy and pre-exponential factor. The latter also depend on the slope of the upwelling path. The competing effects between pressure and temperature on diffusion during upwelling result in reductions in the effective activation enthalpy for diffusion and exchange enthalpy for partitioning, which in turn leads to systematic deviations in closure temperatures from cases of constant pressure. For systems with large activation volume for diffusion, it may be possible to deduce upwelling path and upwelling rate from closure temperatures and closure pressures of selected elements. Examples of closure temperature and closure pressure for REE diffusion in garnet and clinopyroxene and in garnet–clinopyroxene aggregates are presented and discussed in the context of the minor's rule and the REE-in-garnet–clinopyroxene thermobarometer. Closure temperatures for middle-to-heavy REE in garnet–clinopyroxene aggregates are controlled primarily by diffusion in clinopyroxene unless the modal abundance of garnet is very small or the effective grain size of clinopyroxene is considerably smaller than that of garnet.

Keywords Closure temperature · Closure pressure · Closure path · Upwelling path · Cooling · Upwelling · Cooling rate · Upwelling rate · Diffusion · REE diffusion · Garnet · Clinopyroxene · Dodson's equation · REE-in-garnet–clinopyroxene thermobarometer

Introduction

Closure temperature is an important concept to diffusional loss in minerals that experienced cooling (Dodson 1973, 1976, 1986; Albarède 1995; Lasaga 1998; Ganguly and Tirone 1999, 2001; Zhang 2008). It is defined as the lower temperature limit at which the element of interest effectively ceases diffusive exchange with its surrounding medium during cooling. According to Dodson (1973), closure temperature for an element in a mineral grain depends on diffusion parameters of the element and decreases with the decrease of the product of cooling rate and the square

Communicated by Timothy L. Grove.

Electronic supplementary material The online version of this article (doi:10.1007/s00410-016-1327-8) contains supplementary material, which is available to authorized users.

✉ Yan Liang
yan_liang@brown.edu

[1] Department of Earth, Environmental and Planetary Sciences, Brown University, Providence, RI 02912, USA

of effective diffusion radius (d_A). It is given by Dodson's equation

$$\frac{E_A}{RT_c} = G + \ln \frac{D_A^0 R T_c^2}{E_A \dot{s} d_A^2}, \tag{1a}$$

where T_c is the average or mean closure temperature; G is the average of the closure function, depending on geometry of the mineral; E_A and D_A^0 are the activation energy and pre-exponential factor for diffusion of the element of interest in mineral A; $\dot{s}$ is the absolute value of cooling rate at the closure temperature; and R is the gas constant. Equation (1a) can also be written in terms of the diffusion coefficient evaluated at the closure temperature, D_A^c, viz.,

$$\frac{E_A \dot{s}}{RT_c^2} \frac{d_A^2}{D_A^c} = \exp(G), \tag{1b}$$

where terms on the left hand side of Eq. (1b) represent a measure of diffusion time relative to cooling time at the closure temperature. The geometry function, G, in Dodson's equation was modified by Ganguly and Tirone (1999, 2001) to include the "memory effect" that arises from situations when diffusion has not affected the center of the crystal (i.e., cases of fast cooling and large grain size). Powell and White (1995) and Liang (2015) generalized Dodson's equation to bi-mineralic systems. Cherniak and Watson (2007), Gardés and Montel (2009) and Watson and Cherniak (2013) expanded Dodson's equation to more general heating–cooling scenarios.

Many petrologic processes involve changes in both temperature (T) and pressure (P). Consider the thermal history of a mantle parcel M_1 in P–T space in Fig. 1. Initially M_1 was on geotherm H_1 (time = t_1). Between time t_1 and t_2, M_1 was slowly brought to shallower depth along P–T path M_1–N to geotherm H_2. Changes in temperature and pressure would result in redistribution of major and trace elements among minerals in parcel N. If the upwelling rate is slow compared to major element diffusion rates in minerals, the major elements in minerals in parcel N will be homogeneous and their abundances can be used to calculate equilibrium temperature and pressure at N which are independent of its thermal history, i.e., we cannot tell whether N comes from M_1 or M_2 in Fig. 1. If the upwelling rate is faster compared to diffusion rates of certain slow-diffusing cations in the minerals, such as REE in pyroxene or garnet, it may be possible to deduce at least part of the thermal history of N by teasing out temperature, pressure, and rate information encapsulated by the slow diffusing cations in the minerals. For example, temperatures and pressures derived from the abundance and distribution of REE in minerals originated from M_1 and M_2 may correspond to points Q_1 and Q_2 in

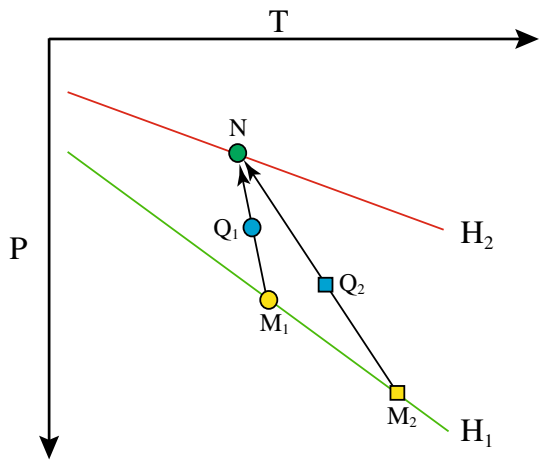

Fig. 1 Schematic diagram illustrating two upwelling paths (M_1–N and M_2–N) in P–T space. Upwelling ends at point N. Q_1 and Q_2 are closure temperatures and closure pressures of a slow diffusing trace element along the two paths, respectively

Fig. 1, while the major element-derived temperatures and pressures are at point N. The direction between N and Q_m ($m = 1$ or 2) maybe related to upwelling trajectory in P–T space (arrows in Fig. 1), while differences in temperature and pressure between N and Q_m may tell us something about the rate or duration of cooling and decompression associated with upwelling.

The effect of changing pressure on diffusional loss or gain in a cooling petrological system has not been considered in Dodson's model. Within the framework of Dodson's formulation, one can include the pressure effect by considering the general Arrhenius equation for diffusion, viz.,

$$D_A(T,P) = D_A^0 \exp\left(-\frac{E_A + PV_A}{RT}\right), \tag{2}$$

where V_A is the activation volume for diffusion of an element in mineral A. The numerator in the Arrhenius equation defines an activation enthalpy for diffusion, i.e., $H_A = E_A + PV_A$. It is tempting to add the pressure effect to Dodson's equation by replacing the activation (internal) energy E_A in Eq. (1a) with the activation enthalpy H_A defined above. Unfortunately, the resultant equation is incomplete in this more general case, as both temperature and pressure in Eq. (2) are functions of time during upwelling.

The chief objective of this study is to quantify the effect of pressure on closure temperature of a trace element in mono-mineralic and bi-mineralic systems that experienced both cooling and decompression. As will be shown below, the generalized Dodson's equation also depends on upwelling path (i.e., M_1–N or M_2–N in

Fig. 1) or upwelling rate (dP/dt) of the cooling petrological system under consideration. For a given closure temperature, there is a corresponding closure pressure. The closure path defined by the closure temperatures and closure pressures follows the upwelling trajectory of the mantle parcel in P–T space. For systems with large activation volume for diffusion, it may be possible to deduce upwelling path and upwelling rate from closure temperatures and closure pressures of selected elements of different mobility.

Closure temperature and closure pressure along a *P–T–t* path

We consider diffusional loss of a trace element in a mineral that moves along the upwelling path M_1–N in Fig. 1 with a prescribed rate. Similar to the diffusional loss problem of Dodson (1973), we assume that (1) diffusion in mineral is isotropic; (2) grain growth and phase transformation are negligible during cooling and decompression; and (3) surrounding medium is effectively an infinite sink or source for the element of interest in the mineral. To include the pressure effect, we first conduct an order of magnitude analysis of diffusional loss by comparing cooling time and diffusive re-equilibration time for the trace element in the mineral following a procedure similar to those of Dodson (1976) and Albarède (1995). In a later section ("Generalization"), we also outline a more rigorous proof of the results described below.

The cooling time constant (τ) is an important concept in closure temperature formulation. According to Dodson (1973), it is defined as the time it takes to decrease the diffusion coefficient D_A for the element of interest in mineral A by a factor of e or 63%, viz.,

$$\tau = -\left(\frac{\mathrm{d}\ln D_A}{\mathrm{d}t}\right)^{-1}, \tag{3}$$

where t is time. For an upwelling parcel such as point Q_1 moving along path M_1–N in Fig. 1, both its pressure and temperature vary as a function of time. From Eq. (2), we have

$$\frac{\mathrm{d}\ln D_A}{\mathrm{d}t} = -\frac{\mathrm{d}}{\mathrm{d}t}\left(\frac{E_A + PV_A}{RT}\right) = \frac{E_A + PV_A}{RT^2}\frac{\mathrm{d}T}{\mathrm{d}t} - \frac{V_A}{RT}\frac{\mathrm{d}P}{\mathrm{d}t}. \tag{4}$$

Since P and T follow path M_1–N, the decompression rate (dP/dt) is related to the cooling rate (dT/dt) through the slope of the upwelling path in P–T space (dP/dT), viz.,

$$\frac{\mathrm{d}P}{\mathrm{d}t} = \left(\frac{\mathrm{d}P}{\mathrm{d}T}\right)_{\text{u-p}}\frac{\mathrm{d}T}{\mathrm{d}t}, \tag{5}$$

where the subscript 'u-p' stands for 'upwelling path' and is used here to emphasize the path-dependent nature of dP/dT. Hence the cooling time constant is path-dependent and given by

$$\tau = \frac{RT^2}{\left\{E_A + \left[P - \left(\frac{\mathrm{d}P}{\mathrm{d}T}\right)_{\text{u-p}}T\right]V_A\right\}\dot{s}}, \tag{6}$$

where $\dot{s} = -dT/dt$ is the cooling rate at a given P and T. All else being equal, the cooling time constant is larger for an upwelling parcel moving along a steeper path than along a shallower path in P–T space (cf. paths M_1–N and M_2–N in Fig. 1).

The characteristic diffusion time (t_D) for an element in mineral A is given by the simple expression

$$t_D = \frac{3\beta d_A^2}{D_A}, \tag{7}$$

where β is a constant, depending on mineral shape and boundary condition; d_A is the effective grain radius. The mineral is effectively closed to diffusional loss to its surrounding when the cooling time is shorter than the diffusion time (Dodson 1976; Albarède 1995; Liang 2015). At closure temperature T_c, Eqs. (6) and (7) differ by a constant factor A', viz.,

$$\frac{d_A^2}{D_A^c} = \frac{A'}{3\beta}\frac{RT_c^2}{\left\{E_A + \left[P_c - \left(\frac{\mathrm{d}P}{\mathrm{d}T}\right)_{\text{u-p}}T_c\right]V_A\right\}\dot{s}}, \tag{8a}$$

where D_A^c is diffusion coefficient at the closure temperature T_c and closure pressure P_c,

$$D_A^c = D_A^0 \exp\left(-\frac{E_A + P_c V_A}{RT_c}\right). \tag{8b}$$

Equation (8a) is the same as Dodson's equation for the mean or grain averaged closure temperature (Eq. 1b) when the average of the geometry function $G = \ln(A'/3\beta)$ and $V_A = 0$ or $dP/dT = 0$. According to Dodson (1986), the mean values of G are 4.0066 for sphere, 3.29506 for cylinder, and 2.15821 for plane sheet.

The closure temperature and closure pressure in Eq. (8a) are related to each other through the upwelling path. For purpose of demonstration, here we consider a linear path of the form (e.g., M_1–N in Fig. 1),

$$P_c = P_{ref} + \left(\frac{\mathrm{d}P}{\mathrm{d}T}\right)_{\text{u-p}}(T_c - T_{ref}), \tag{8c}$$

where P_{ref} and T_{ref} are the pressure and temperature at a reference point along the linear upwelling path. Without loss of generality, we use the pressure and temperature at point

N (P_N and T_N) in Fig. 1 in the formulations below. Substituting Eq. (8c) into Eq. (8a), we have a generalized expression for the mean closure temperature of a trace element in the cooling-upwelling mono-mineralic system,

$$\frac{H_A^{\text{u-p}}\dot{s}}{RT_c^2}\frac{d_A^2}{D_A^c} = \exp(G), \tag{9a}$$

where $H_A^{\text{u-p}}$ is a path-dependent activation enthalpy for diffusion in mineral A,

$$H_A^{\text{u-p}} = E_A + \left[P_N - \left(\frac{\mathrm{d}P}{\mathrm{d}T}\right)_{\text{u-p}} T_N\right] V_A, \tag{9b}$$

D_A^c, which is the diffusion coefficient evaluated at T_c and P_c, can also be written as

$$D_A^c = D_A^{0,\text{u-p}} \exp\left(-\frac{H_A^{\text{u-p}}}{RT_c}\right), \tag{9c}$$

where $D_A^{0,\text{u-p}}$ is a path-dependent pre-experiential factor for diffusion,

$$D_A^{0,\text{u-p}} = D_A^0 \exp\left[-\frac{V_A}{R}\left(\frac{\mathrm{d}P}{\mathrm{d}T}\right)_{\text{u-p}}\right]. \tag{9d}$$

For the linear upwelling path considered here, the second term on the right-hand side of Eq. (9b) is independent of the choice of the reference pressure and temperature so long as they are on the upwelling path. For example, one can use temperatures and pressures derived from major element-based thermobarometers to represent T_N and P_N in Eq. (9b). Given T_N and P_N, cooling rate, and slope of the upwelling path, the closure temperature can be solved from Eq. (9a) numerically using standard method. The closure pressure is given by Eq. (8c).

Discussion

Comparison with Dodson's model

Equation (9a) has the same form as Dodson's equation (cf. Eq. 1b) if one replaces the activation energy and pre-exponential factor for diffusion in Dodson's equation by the path-dependent activation enthalpy (Eq. 9b) and pre-experiential factor (Eq. 9d). Equation (9a) reduces to Dodson's equation (Eq. 1b) in the absence of upwelling (i.e., when $\mathrm{d}P/\mathrm{d}T = 0$ in Eqs. 9b–9d) or when diffusion in mineral A is insensitive to pressure (i.e., $V_A = 0$).

Few studies focus on effect of pressure on cation diffusion in minerals. Published tracer diffusion data (see reviews in Béjina et al. 2003; Chakraborty 2010) suggest activation energies are positive and vary from less than 1×10^{-6} m^3/mol (weak pressure dependence) to 20×10^{-6} m^3/mol (strong pressure dependence). The exception is an earlier study by Sneeringer et al. (1984) in which they reported negative activation energies for Sr diffusion in diopside. Cherniak and Watson (2012) measured He diffusion in olivine at 0.1 MPa and 2.7 GPa and could not detect any change in measured diffusivity with pressure. Van Orman et al. (2001) measured Ce and Yb diffusion in diopside at pressures of 0.1 MPa to 2.5 GPa and reported activation volumes of $10.2\pm3.2\times10^{-6}$ and $9.5\pm2.0\times10^{-6}$ m^3/mol, respectively. There are some uncertainties in quantifying pressure-dependent REE diffusion in garnet. Bloch et al. (2015) measured Lu diffusion coefficient in natural almandine and spessartine over a range of P, T, and oxygen fugacity, and reported an activation volume of $10.6\pm1.02\times10^{-6}$ m^3/mol. Based on laboratory measured diffusion coefficients of REE and Y in grossular at 0.1 MPa (Cherniak 2005) and pyrope at 2.8 GPa (Van Orman et al. 2002b) and stranded diffusion profiles in natural garnets (modeled at 0.53 GPa), Carlson (2012) obtained a general Arrhenius expression for REE diffusion in garnet over a range of P, T, oxygen fugacity, and garnet composition. He found an activation volume for REE diffusion in garnet of $20.75\pm0.66\times10^{-6}$ m^3/mol. Including the newer data from Bloch et al. (2015) in a rigorous statistical analysis of REE diffusion in garnet, Chu and Ague (2015a) did not find a decrease in the estimated activation volume for REE diffusion in garnet (Chu personal communication, 2016). The uncertainties in the activation volume may be due, in part, to the limited

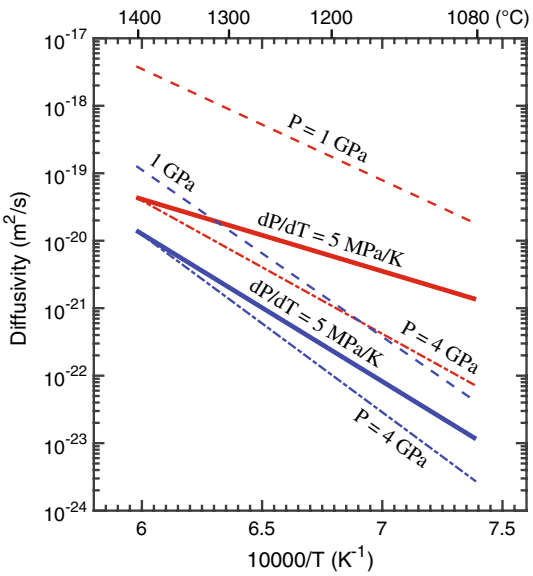

Fig. 2 Diffusion coefficients of Ce in garnet (*red lines*) and diopside (*blue lines*) at constant pressures of 1 and 4 GPa and along a linear upwelling path with a slope of 5 MPa/K. Diffusion parameters for diopside and garnet are from Van Orman et al. (2002a) and Carlson (2012), respectively

number of high-pressure experiments for REE diffusion in garnet: 6 at 2.8 GPa (Van Orman et al. 2002b), 1 at 1.9 GPa and 1 at 3.4 GPa (Bloch et al. 2015), different garnets used in the experiments, and/or method in retrieving diffusion coefficients. In spite of the uncertainties in the activation volume, pressure has a moderate-to-strong effect on REE diffusion in garnet and diopside. This is illustrated in Fig. 2.

In general, diffusion coefficients increase with the increase of temperature and the decrease of pressure. Hence there is a competing effect between temperature and pressure on cation diffusion in minerals along a geotherm (e.g., Holzapfel et al. 2007; Watson and Baxter 2007). Figure 2 compares diffusion coefficients of Ce in diopside and garnet at two selected pressures (1 and 4 GPa, dashed lines) and along an upwelling path that passes through 1400 °C and 4 GPa with a slope of 5 MPa/K (solid lines). Diffusion coefficients were calculated using parameters reported in Van Orman et al. (2002a) for diopside and Carlson (2012) for garnet. At 1300 °C, diffusivities of Ce in diopside and garnet at 1 GPa are one and two orders of magnitude of the respective values at 4 GPa (one order of magnitude if an activation volume of 10×10^{-6} m^3/mol is used for garnet). These differences become even larger at lower temperatures (Fig. 2). In the case of upwelling, the relatively large and positive activation energies for REE diffusion in diopside and garnet work against the dominant effect of decreasing temperature, resulting in a reduction in the apparent activation enthalpy for diffusion, i.e.,

$$E_A + PV_A = \underline{E_A + P_{ref}}V_A + \left(\frac{\mathrm{d}P}{\mathrm{d}T}\right)_{\text{u-p}}\left(T - T_{ref}\right)V_A, \qquad (10)$$

where the first two terms on the right-hand side of Eq. (10) is the activation energy at the reference pressure, P_{ref}. For the case of P_{ref} = 4 GPa and T_{ref} = 1400 °C, the last term in Eq. (10) is negative. Hence the steeper the upwelling trajectory in *P–T* space, the larger the activation enthalpy reduction and the lesser the decrease of the diffusivities with falling temperature will be. Interestingly, if we

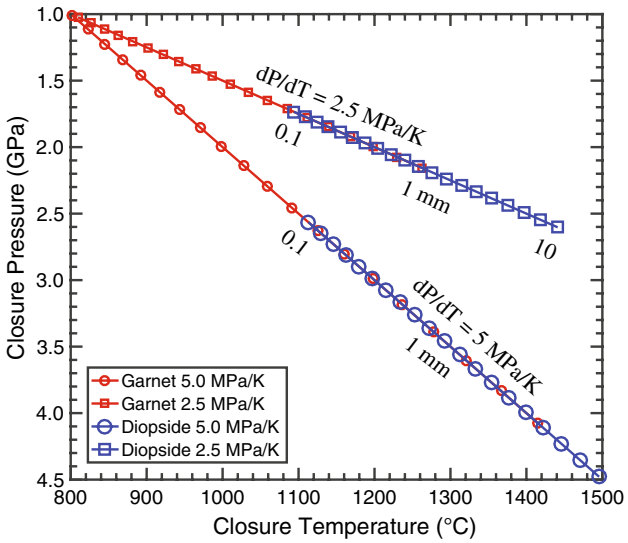

Fig. 4 Closure paths defined by the closure temperatures and closure pressures of Ce in garnet (*red symbols*) and diopside (*blue symbols*) for a range of effective grain sizes (20 data points for each case, same as those used in Fig. 3). Minerals with larger grain size and smaller diffusivity are closed at higher temperatures and pressures

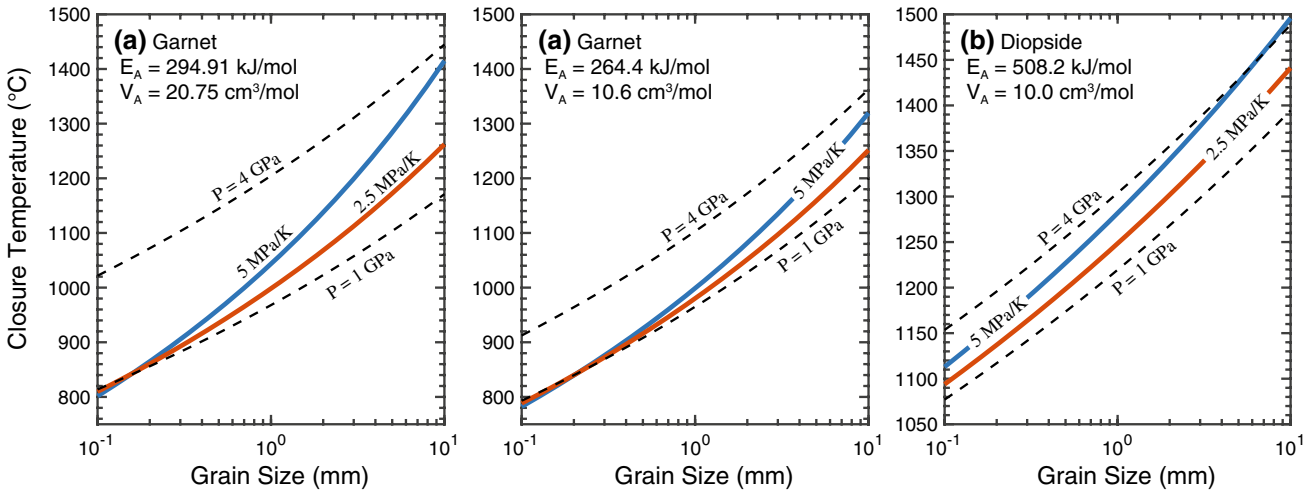

Fig. 3 Variations of closure temperatures of Ce in garnet (**a, b**) and diopside (**c**) as a function of effective diffusion radius at a cooling rate of 100 °C/Myr along two upwelling paths (*solid lines*). For comparison, closure temperatures at constant pressures of 1 and 4 GPa are also shown as dashed lines. Diffusion parameters for diopside are from Van Orman et al. (2002a). Diffusion parameters for garnet in **a** are from Carlson (2012). Diffusion parameters for Ce in garnet in **b** are assumed to be the same as those for Lu in garnet from Bloch et al. (2015)

double the slope of upwelling path for the case in Fig. 2 ($dP/dT = 10$ MPa/K), diffusivity of Ce in garnet becomes almost independent of temperature.

Figure 3a–c displays closure temperatures of Ce in garnet and diopside as a function of effective diffusion radius for a cooling rate of 100 °C/Myr and two choices of upwelling paths (Fig. 4) calculated using Eq. (9a) and diffusion parameters listed in Van Orman et al. (2002a), Carlson (2012), and Bloch et al. (2015). For comparison, closure temperatures calculated using Dodson's equation (Eq. 1b) at constant pressures of 1 and 4 GPa are also shown (dashed lines). For a given grain size, closure temperatures at a constant pressure of 4 GPa are considerably higher than those at 1 GPa, by more than 200 (or 100) °C for garnet and 70–100 °C for diopside. This is due mainly to the difference in activation volume for diffusion between the two minerals (the differences in slope between the two minerals in Fig. 3 for the isobaric cases are due to the difference in activation energy between garnet and diopside). Figure 3a, b also highlights the importance of activation volume for diffusion: a reduction of activation volume by half results in a decrease in the isobaric closure temperature by ~100 °C for REE in garnet (~50 °C for diopside, supplementary Fig. S1a and S1b). The closure temperature is practically independent of pressure when the activation volume for diffusion is $\leq 1 \times 10^{-6}$ m^3/mol (supplementary Fig. S1c and S1d).

Equations (9a–9d) indicate that closure temperature depends on cooling and decompression path. During upwelling, the competing effects of pressure and temperature on diffusion drive closure temperature along the upwelling path. Since larger grains close at higher temperatures, their closure pressures are also high, which results in higher apparent activation enthalpy for diffusion at the closure and hence the larger slope in the plot of closure temperature vs. effective grain size. This is illustrated in Fig. 3 for two choices of upwelling paths. The closure temperatures approach and even exceed Dodson's 4 GPa curve for large enough grain size, but converge and pass below Dodson's 1 GPa curve for smaller grain size with reduced slopes in these diagrams. For a given cooling rate, the steeper the slope of the upwelling path (dP/dT), the faster the upwelling rate is (Eq. 5), and the higher the closure temperature will be (cf. blue and red lines in Fig. 3). For minerals with larger activation volume for diffusion, their closure temperatures are more sensitive to upwelling path (cf. Fig. 3a, b and supplementary Fig. S1a–1c). Hence effect of pressure on closure temperature is significant when the activation volume for diffusion is large and the slope of upwelling path is steep.

Figure 4 displays closure temperatures and closure pressures for the four upwelling cases considered in Fig. 3a, c. Although garnet and diopside are closed to diffusional loss at different temperatures and pressures for a given grain size and upwelling slope (cf. Fig. 3a, c), closure temperatures and closure pressures for the two minerals follow the upwelling paths for the same geothermal gradient via Equation (8c). Here for purpose of demonstration, we choose $P_{ref} = 1$ GPa and $T_{ref} = 800$ °C. Figure 4 also shows that closure temperatures and closure pressures for a mineral with different grain size fall along the upwelling path. This is an important feature of diffusional loss along an upwelling path and has been independently verified by numerical solutions of diffusion equations under similar settings (Yao 2015). Hence it may be possible to deduce upwelling trajectory of a group of petrologically related igneous and metamorphic rocks by comparing their closure temperatures and closure pressures for fine-grained and coarse-grained samples.

Finally, we note that closure temperature depends on the product of cooling rate and grain size squared ($\dot{s}d^2$) in all the closure temperature equations. Hence examples presented in Figs. 3, 4, 5, 6 and 7 (and supplementary figures) for a constant cooling rate of 100 °C/Myr can also be rescaled to other cooling rates by adjusting the effective grain size in the equations accordingly. Furthermore, diffusivities of REE in diopside and garnet vary systematically with their ionic radii (Van Orman et al. 2001; Carlson 2012). Hence observations derived from diffusive behavior of Ce are also applicable to other REE in the two minerals, as we will further illustrate in the next section.

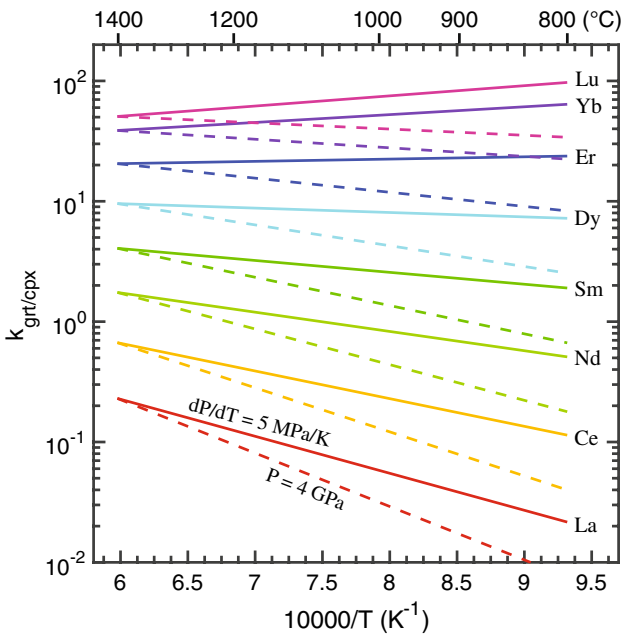

Fig. 5 Variations of garnet–clinopyroxene REE partition coefficients along two *P–T* paths. Arrhenius parameters are listed in supplementary Table S1

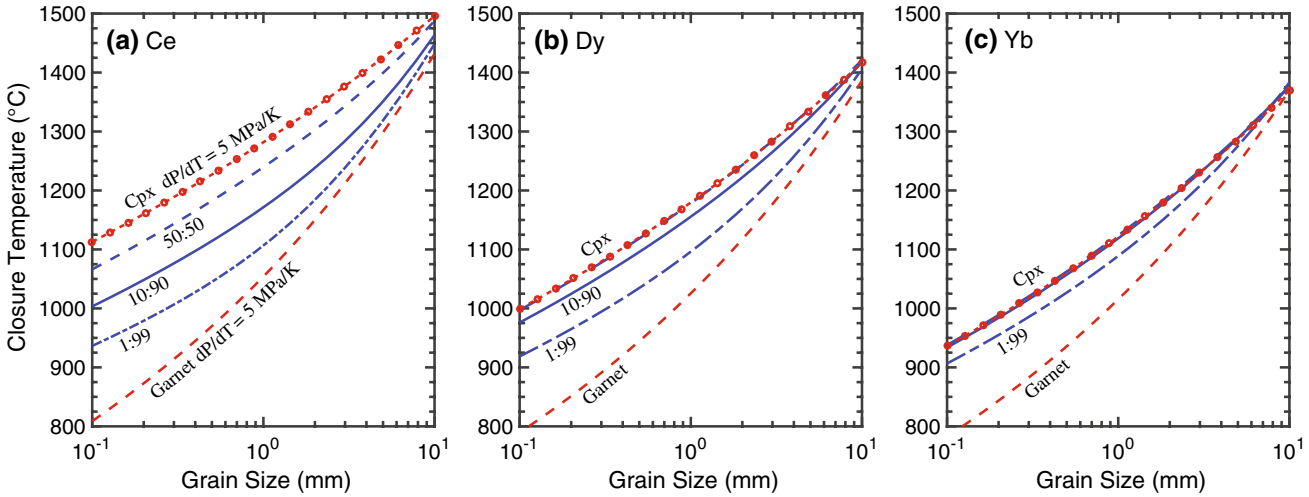

Fig. 6 Variations of closure temperatures of Ce (**a**), Dy (**b**), and Yb (**c**) in three garnet + clinopyroxene aggregates as a function of effective diffusion radius along two upwelling paths at a cooling rate of 100 °C/Myr. For comparison, closure temperatures of the respective elements in garnet (*dashed lines*) and clinopyroxene (Cpx, *dashed line* with *small circles*) along the same upwelling path are also shown. Diffusion parameters for clinopyroxene and garnet are from Van Orman et al. (2002a) and Carlson (2012), respectively

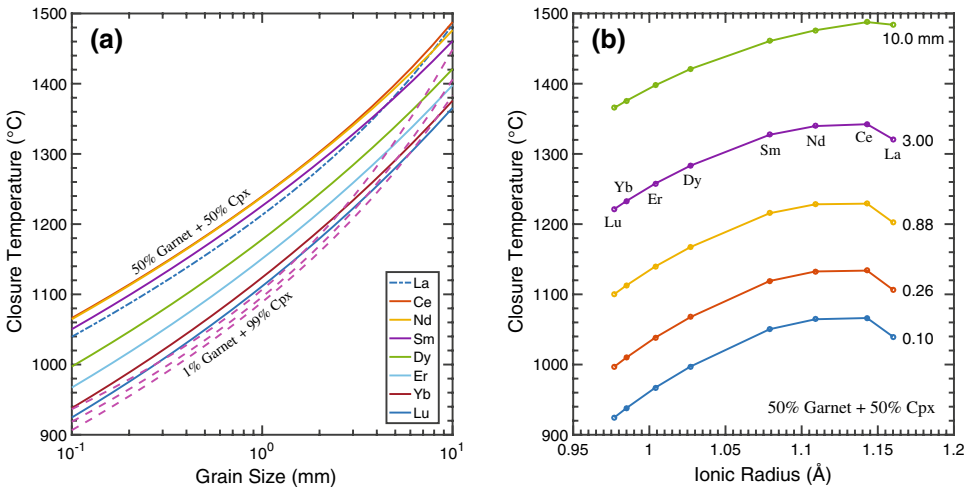

Fig. 7 Variations of closure temperatures of selected REE in a 50% garnet + 50% clinopyroxene aggregate as a function of effective diffusion radius (**a**) and trivalent REE ionic radius (**b**) along an upwelling path ($dP/dT = 5$ MPa/K) at a cooling rate of 100 °C/Myr. For comparison, closure temperatures of Ce, Dy, and Yb for the 1% garnet + 99% clinopyroxene aggregate are shown as *red dashed lines* in **a**. Diffusion parameters for clinopyroxene and garnet are from Van Orman et al. (2002a) and Carlson (2012), respectively

Generalization

To highlight the role of pressure in diffusional loss during upwelling, we used a simple order of magnitude analysis to identify key parameters controlling closure temperature and closure pressure in cooling-upwelling mono-mineralic systems. This simple method leads to an equation that differs from Dodson's closure temperature expression by a constant factor. To constrain the constant, solutions of the diffusion equations are needed. Here we show that the path-dependent Eqs. (9a–9d) for closure temperature and closure pressure can indeed be derived from a more rigorous analysis of the diffusion equations for the case of linear upwelling path (Fig. 1).

Without loss of generality, we consider diffusional loss of an element in a spherical mineral grain of radius d. In axial symmetric coordinate, the diffusion equation and boundary conditions for the element of interest in the mineral (concentration C_A) take on the usual expressions,

$$\frac{\partial C_A}{\partial t} = D_A(T,P)\left(\frac{\partial^2 C_A}{\partial r^2} + \frac{2}{r}\frac{\partial C_A}{\partial r}\right), \tag{11a}$$

$$C_A(d,t) = C_A^0(T,P), \tag{11b}$$

$$\left.\frac{\partial C_A}{\partial r}\right|_{r=0} = 0, \tag{11c}$$

where $C_A^0(T,P)$ is the concentration on the mineral surface. The temperature- and pressure-dependent diffusion coefficient, $D_A(T, P)$, is given by the Arrhenius equation for diffusion (Eq. 2). When T and P are functions of time, the diffusion coefficient varies with time. Equations (11a–11c) can be simplified by introducing a new time variable u (Dodson 1973),

$$u = \int_0^t D_A[T(t'), P(t')]\mathrm{d}t'. \tag{12}$$

At a constant pressure, $P = P_0$, and a prescribed cooling rate, Dodson (1973) obtained an analytical solution to Eqs. (11a–11c) and used the solution to construct an expression for closure temperature (e.g., Eq. 1). Since diffusion rate generally decreases with increasing pressure, one can, in principle, define a closure pressure P_c at a constant temperate, $T = T_0$, and a prescribed compression rate following the procedures outlined in Dodson (1973, 1976).

When both T and P vary with time, the closure temperature and closure pressure are related to each other through the closure time along the P–T–t path experienced by the mineral. During upwelling, the pressure of the parcel is related to its temperature through the linear expression,

$$P = P_{ref} + \left(\frac{\mathrm{d}P}{\mathrm{d}T}\right)_{\text{u-p}}\left(T - T_{ref}\right). \tag{13}$$

Substituting Eq. 13 into the pressure- and temperature-dependent Arrhenius equation (Eq. 2), we have a pressure-free Arrhenius expression for diffusivity of an element in mineral A along the upwelling path,

$$D_A(T) = D_A^{0,\text{u-p}} \exp\left(-\frac{H_A^{\text{u-p}}}{RT}\right), \tag{14a}$$

where $D_A^{0,\text{u-p}}$ and $H_A^{\text{u-p}}$ are shorthand notations for the path-dependent pre-exponential factor and activation enthalpy for diffusion:

$$D_A^{0,\text{u-p}} = D_A^0 \exp\left[-\frac{V_A}{R}\left(\frac{\mathrm{d}P}{\mathrm{d}T}\right)_{\text{u-p}}\right], \tag{14b}$$

$$H_A^{\text{u-p}} = E_A + \left[P_{ref} - \left(\frac{\mathrm{d}P}{\mathrm{d}T}\right)_{\text{u-p}} T_{ref}\right] V_A \tag{14c}$$

Given Eqs. (14a–14c), one can solve the diffusion equation with time-dependent diffusion coefficient (e.g., Eqs. 11a–11c) following steps outlined in Dodson (1973) and obtain the path-dependent closure temperature equation (Eq. 9a) for upwelling along the linear P–T path described by Eq. (13). Since Eq. (14a) is the only change needed to account for upwelling and the upwelling rate is related to geothermal gradient via Eq. (5), we can make the following general statement regarding closure temperature equations for cooling petrological systems:

> To include linear upwelling in a Dodson-type closure temperature equation, one simply replaces the pre-exponential factor and activation energy for diffusion in the original isobaric equation by the path-dependent exponential factor and activation energy for diffusion while keeping the other terms unchanged in the original equation.

The generalized closure temperature equation of Ganguly and Tirone (1999, 2001) for systems with arbitrarily small amount of diffusion, for example, now takes on the form,

$$\frac{H_A^{\text{u-p}}}{RT_c(x)} = \frac{H_A^{\text{u-p}}}{RT_0} + \ln\frac{RD_A\left(T_0\right)T_c^2(x)}{H_A^{\text{u-p}}\dot{s}d_A^2} + G(x) + g(x), \tag{15}$$

where $T_c(x)$ is the closure temperature profile; x is the distance measured from the center of the grain; $D_A\left(T_0\right)$ is the diffusion coefficient evaluated at the peak temperature and pressure (T_0 and P_0), i.e., at the onset of upwelling; $G(x)$ and $g(x)$ are spatial-dependent closure function and memory function, respectively. Expressions and averaged values of $G(x)$ and $g(x)$ can be found in Dodson (1986) and Ganguly and Tirone (1999, 2001). Following the basic idea of Dodson (1973), Cherniak and Watson (2007) and Gardés and Montel (2009) considered diffusive "opening" during heating, and Watson and Cherniak (2013) provided general equations for both heating alone and thermal pulses. Their resultant expressions for diffusive opening at constant pressure can also be generalized to include compression or subduction along a linear path in P–T space using the substitutions outlined above.

Powell and White (1995) and Liang (2015) presented algebraic equations for closure temperature in cooling bi-mineralic systems that have not been affected by open system mass transfer processes. Here the closure temperature is referred to the temperature at which the trace element of interest is effectively ceased diffusive exchange between the two minerals in a closed system. In addition to diffusion parameters, closure temperature in cooling bi-mineralic systems depends on partition coefficient of the element between the two minerals as well as their relative proportions. For a trace element, its pressure- and temperature-dependent mineral–mineral partition coefficient, k_{AB}, takes on the general form,

$$k_{AB}(T,P) = k_{AB}^0 \exp\left(-\frac{E_k + PV_k}{RT}\right), \tag{16}$$

where E_k, V_k, and k_{AB}^0 are the exchange energy, exchange volume, and pre-exponential factor for the partitioning of

the trace element between mineral A and mineral B. For a linear upwelling path, the pressure in Eq. (16) can be replaced by temperature via Equation (13), viz.,

$$k_{AB}(T) = k_{AB}^{0,\text{u-p}} \exp\left(-\frac{H_k^{\text{u-p}}}{RT}\right), \tag{17a}$$

$$k_{AB}^{0,\text{u-p}} = k_{AB}^{0} \exp\left[-\frac{V_k}{R}\left(\frac{\mathrm{d}P}{\mathrm{d}T}\right)_{\text{u-p}}\right], \tag{17b}$$

$$H_k^{\text{u-p}} = E_k + \left[P_{ref} - \left(\frac{\mathrm{d}P}{\mathrm{d}T}\right)_{\text{u-p}} T_{ref}\right] V_k. \tag{17c}$$

An algebraic equation for the mean closure temperature and closure pressure of a trace element in bi-mineralic systems that experience cooling and decompression along a linear P–T path is presented in the Appendix 1 (Eq. 18) along with a brief description. This equation is reduced to Eq. (9a) for mineral A when the volume fraction of A is very small and the abundance of the element of interest in A is much smaller than that in B (i.e., when mineral B serves as an effectively infinite sink or source for the element of interest in the bi-mineralic system).

As an illustrated example, we consider mean closure temperatures and closure pressures of REE in cooling-upwelling bi-mineralic systems consisting of garnet and clinopyroxene, that is, the temperatures and pressures at which diffusive exchanges of REE between garnet and clinopyroxene are effectively stopped in the closed system. Partitioning of REE between garnet and clinopyroxene depends on temperature, pressure and mineral major element compositions (Sun and Liang 2014). For comparison, here we consider two garnet–clinopyroxene pairs: one from a diamond eclogite (sample JDE22 in Smart et al. 2009) and the other from a garnet peridotite (sample Pra33 in Bjerg et al. 2009). For simplicity, we use the parameterized lattice strain model of Sun and Liang (2014) to calculate REE partition coefficients as a function of P and T while keeping major element compositions of the minerals fixed. In a more realistic scenario, major element compositions of coexisting garnet and clinopyroxene also change as a function of temperature and pressure. Table S1 in supplementary material listed the partitioning parameters for the two samples. The exchange energies (E_k) vary systematically as a function of ionic radius, 78–80 kJ/mol for La, 30–32 kJ/mol for Gd, and −0.4 to −2.6 kJ/mol for Lu, while the exchange volume (V_k) is nearly constant with an average value of 3.2×10^{-6} m^3/mol. Figure 5 displays selected REE partition coefficients between garnet and clinopyroxene along the 5 MPa/K P–T path shown in Fig. 4 for the eclogite (a similar figure for the garnet peridotite is presented in supplementary Figure S2). In both cases, La and Ce are moderately to highly incompatible, while Sm to Lu are compatible to highly compatible in garnet relative to clinopyroxene. The competing effect of decreasing temperature and pressure along the upwelling path gradually elevates garnet/clinopyroxene REE partition coefficients (cf. solid and dashed lines in Fig. 5 and Fig. S2), resulting in negative apparent exchange energies for Er, Yb and Lu partitioning along the geotherm (i.e., positive slopes in these figures). These have interesting implications for diffusive re-equilibration of REE between garnet and clinopyroxene.

Figure 6a–c displays closure temperatures of Ce, Dy and Yb in garnet + clinopyroxene aggregates as a function of effective diffusion radius for three choices of garnet:clinopyroxene volume proportions (50:50, 10:90 and 1:99), a cooling rate of 100 °C/Myr and an upwelling gradient $\mathrm{d}P/\mathrm{d}T = 5$ MPa/K. Figure 7a, b compares closure temperatures of selected REE as functions of ionic radius and effective grain sizes. For purpose of illustration, we set the grain size of garnet the same as that of clinopyroxene ($d_{\text{garnet}} = d_{\text{cpx}}$) and used the diffusion parameters from Carlson (2012) for garnet. Four interesting observations can be readily made from Figs. 6 and 7. First, closure temperatures of REE in the cooling-upwelling garnet + clinopyroxene aggregates are bracketed by the closure temperatures of REE in garnet and clinopyroxene along the same P–T path (red dashed lines in Fig. 6) and closure temperatures along a cooling-upwelling path are different from those at a constant pressure (not shown but cf. Figs. 3, 6a). These are common features for diffusive redistribution of trace element in bi-mineralic systems that are closed to mass exchange with their surrounding. Second, for garnet + clinopyroxene aggregates with more than 5% garnet, closure temperatures of middle to heavy REE are determined primarily by those in clinopyroxene (Fig. 6b, c). Third, closure temperatures of La and Ce are sensitive to garnet:clinopyroxene proportions, especially for systems with less than 50% garnet (Figs. 6a, 7a). And finally, except for systems with very large grain size ($d_{\text{garnet}} = d_{\text{cpx}}$ >8 mm), closure temperatures of La are lower than closure temperatures of Ce and Nd, while closure temperatures of Nd are nearly identical to those of Ce (Fig. 7a, b). In supplementary material, we present diagrams similar to Figs. 5, 6 and 7 for garnet and clinopyroxene in a garnet peridotite calculated using major element compositions reported in Bjerg et al. (2009, their sample Pra33, Figures S2–S4) and for garnet and clinopyroxene in the eclogite sample but with the activation volume for REE diffusion in garnet reduced by half (Figures S5, S6). The four observations described above appear to be common features shared by eclogites and garnet peridotites, insensitive to the choice of activation volume for REE diffusion in garnet (i.e., 20×10^{-6} vs. 10×10^{-6} m^3/mol). These shared features originate from diffusive and partitioning behaviors of REE in garnet and clinopyroxene.

The systematic variations in closure temperature illustrated in Figs. 6 and 7 (and supplementary Figures S3–S6) can be understood in terms of the minor's rule for diffusive re-equilibration in bi-mineralic systems: the mineral that contains a lesser amount of the trace element of interest in the closed system contributes more to the overall diffusive time and hence the closure temperature in the bi-mineralic system (Liang 2014, 2015). The middle-to-heavy REE are highly compatible in garnet relative to clinopyroxene, whereas La and Ce are highly incompatible in garnet (Figs. 5, S2). With considerably higher abundances of middle-to-heavy REE, garnet serves effectively as a very large reservoir for these REE in the garnet–clinopyroxene system, leaving clinopyroxene as the "minor phase" that controls the time scale of diffusion for the middle-to-heavy REE in the bi-mineralic system. Since diffusion of REE in clinopyroxene depends strongly on their ionic radii (Van Orman et al. 2001, 2002a), this also explains the ionic size-dependent behavior of the closure temperatures for the case of 50% garnet + 50% clinopyroxene shown in Fig. 7 (and Figs. S4, S6). Garnet is important to middle-to-heavy REE when its volume fraction is very small (<1%). In contrast, La and Ce budgets in garnet + clinopyroxene aggregates are controlled mainly by clinopyroxene (Fig. 5) except when the clinopyroxene volume fraction is very small. This explains the more prominent role of garnet in determining their closure temperatures in bi-mineral eclogites with less than 50% garnet. In fact, garnet exerts such a strong control on the diffusive re-equilibration time scale of La in the garnet + clinopyroxene aggregates, closures temperatures of La are weighted more towards the closure temperatures of La in garnet, which explains the lower values of the La closure temperatures in Fig. 7 (and Figs. S4, S6).

Nonlinear upwelling path in *P–T* space

For algebraic simplicity, we considered linear upwelling path in *P–T* space in our analysis of the pressure effect. *P–T–t* paths of natural samples are more complicated even for cases involving simple exhumation (e.g., Grasemann et al. 1998; Guillot et al. 2009). Yao (2015) conducted numerical simulations of diffusive re-equilibration of REE between garnet and clinopyroxene during cooling and decompression along parabolic paths in *P–T* space. She showed that the numerically derived closure temperatures and closure pressures, calculated from closure times defined by Dodson (1973, 1976), follow the parabolic *P–T* trajectory in a manner similar to that shown in Fig. 4. In Appendix 2, we present equations for the mean closure temperature and closure pressure along two nonlinear upwelling paths: (a) $P = f(T)$, where $f(T)$ is an arbitrary function of temperature; and (b) $T = c_1 P + c_2 P^2$, where c_1 and c_2 are constants.

Summary and further discussion

Pressure may play an important role during diffusional loss along an upwelling path. Dodson's equation and Dodson-type closure temperature equations for cooling mono-mineralic and bi-mineralic systems are generalized to include the pressure effect by noting that the pressure is related to the temperature through the upwelling path in *P–T* space. For the linear path considered in this study, the resultant closure temperature equations have the same algebraic form as the Dodson-type equations at constant pressure except the diffusion and mineral–mineral partitioning parameters in the generalized equations are path-dependent and can be quantified by considering the slope of the upwelling path. During upwelling, the competing effect of pressure and temperature gives rise to reductions in the apparent activation energy and exchange energy for diffusion and partitioning, which result in systematic deviations in closure temperatures from their isobaric values. For typical activation energies of 300–500 kJ/mol for cation diffusion in minerals, the effect of pressure is important when the activation volume is $\geq 5 \times 10^{-6}$ m^3/mol. This includes REE diffusion in garnet and diopside (Van Orman et al. 2001, 2002a; Carlson 2012; Bloch et al. 2015), and divalent cation diffusion in garnet and olivine (e.g., Chakraborty and Ganguly 1992; Freer and Edwards 1999; Holzapfel et al. 2007; Chu and Ague 2015b). The effect of pressure is especially important when the upwelling rate is high and the slope of upwelling path is large. At present, few data are available for the activation volume and exchange volume of geochemically important elements in minerals of petrologic importance. Results from the present study demonstrate the usefulness of such data in unraveling thermal and tectonic history of igneous and metamorphic rocks.

For a given closure temperature, there is a corresponding closure pressure on the upwelling path. An element that has a higher closure temperature in a mineral assemblage (due to larger grain size or/and slower diffusion) also has a higher closure pressure. For a given element, its closure temperatures and closure pressures in a suite of tectonically related rocks of variable texture (e.g., fine and coarse grain sizes) and composition may be related to each other through the upwelling path. For an uplifted rock that has not been affected by open system processes after its formation, closure temperatures and closure pressures of cations of different mobility and compatibility in its constituent minerals define a *P–T* trajectory that also follows the upwelling path. This conclusion also applies to nonlinear upwelling paths. Hence it may be possible to deduce at least part of upwelling trajectory of igneous and metamorphics rocks by comparing their closure temperatures and closure pressures in *P–T* space. As an example, we compare temperatures and pressures of two garnet peridotites calculated using the

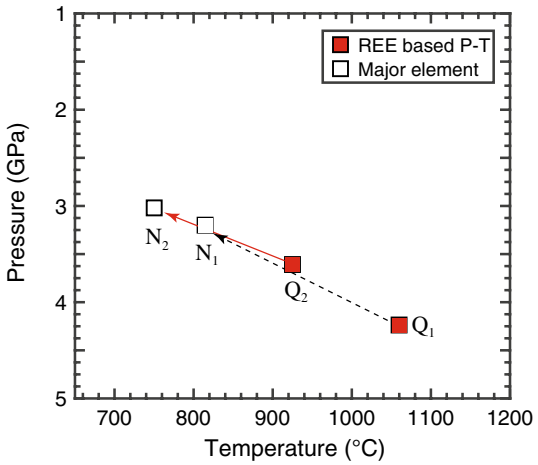

Fig. 8 Upwelling trajectories defined by temperatures and pressures recorded in major elements and REE in coexisting garnet and pyroxenes in two garnetites in garnet peridotites from Otrøy, western Norway. The major element-derived temperatures and pressures are calculated using the thermobarometers of Brey and Köhler (1990, points N_1 and N_2), while REE-based temperatures and pressures are calculated using the REE-in-garnet–clinopyroxene thermobarometer of Sun and Liang (2015, points, Q_1 and Q_2). *Lines with arrows* mark possible upwelling paths. Major element and REE compositions are from Spengler et al. (2006)

REE-in-garnet–clinopyroxene thermobarometer of Sun and Liang (2015) and major element-based thermobarometers that have been widely used in the literature in Fig. 8.

Through numerical simulations of diffusive re-equilibration of REE between garnet and clinopyroxene during cooling and decompression along parabolic paths in *P–T* space, Yao (2015) showed that the apparent temperatures and pressures calculated using the grain-scale averaged REE concentrations in garnet and clinopyroxene and the REE-in-garnet–clinopyroxene thermobarometer are equivalent to the average closure temperatures and closure pressures of REE calculated according to the definition of Dodson (1973, 1976) in the garnet + clinopyroxene aggregates. Figure 8 displays the average closure temperatures and closure pressures of REE for two majoritic garnets with pyroxene exsolutions from Otrøy, western Norway (points Q_1 and Q_2, major and trace element data from Spengler et al. 2006). Also shown are temperatures and pressures calculated using the two-pyroxene thermometer and the Al-in-orthopyroxene barometer of Brey and Köhler (1990, points N_1 and N_2). Based on the presence of oriented intracrystalline pyroxenes exsolved from garnet, depleted light REE patterns in garnet and exsolved pyroxenes, and Nd mineral cooling age, Spengler et al. (2006) deduced the thermal and tectonic history of the Otrøy peridotites that involves decompressional melting of transition zone mantle in the Archaean, followed by either nearly isobaric cooling at the base of the lithosphere till Proterozoic (their Model 1) or a more complicated history that involves subduction or delamination followed by buoyancy-driven upwelling to the base of the lithosphere (their Model 2). In both models, cooling and decompression resulted in closure of the Sm–Nd isotopic system. The closure temperatures and closure pressures deduced from the REE-in-garnet–clinopyroxene thermobarometer (points Q_1 and Q_2 in Fig. 8) may correspond to the 1.4 Ga "Nd mineral cooling time" reported in Spengler et al. (2006). The major element-based temperatures and pressures (points N_1 and N_2 in Fig. 8) correspond to further cooling during decompression until Phanerozoic (stage D in their Fig. 3). Hence the vectors $Q_1 \rightarrow N_1$ and $Q_2 \rightarrow N_2$ in Fig. 8 may be interpreted as part of the upwelling trajectories recorded by the two garnet peridotites. This is consistent with the model of Spengler et al. (2006, stages C and D in their Fig. 3). With detailed thermodynamic modeling of mineral stabilities and diffusion modeling of major element and REE zoning patterns in garnet and pyroxene following *P–T–t* paths, it may be possible to deduce cooling and upwelling rates experienced by these rocks (e.g., Müller et al. 2015; Yao 2015).

Acknowledgements I would like to thank Chenguang Sun for Fig. 8 and the Arrhenius parameters for REE partitioning between garnet and clinopyroxene used in this study, Xu Chu for sharing his unpublished diffusion parameters for REE diffusion in garnet, and Lijing Yao for useful discussion. This paper has benefited from thoughtful review comments by Bruce Watson and Jiba Ganguly. This work was supported in part by NSF Grants EAR-1624516 and EAR-1632815.

Appendix 1: Closure temperature and closure pressure for cooling-upwelling bi-mineralic systems

The analysis outlined in the main text can be easily extended to bi-mineralic systems that experience both cooling and decompression. Here we consider diffusive exchange of a trace element in a cooling-upwelling bi-mineralic aggregate in a representative elementary volume or REV along a *P–T–t* path (Fig. 1). The bi-mineralic aggregate consists of minerals *A* and *B* of average half sizes or radii d_A and d_B and volume fractions φ_A and φ_B, respectively, in the REV. In addition to the three assumptions for the mono-mineralic systems, we assume that (4) the two minerals are in local equilibrium at their interfaces; and (5) grain boundary diffusion is much faster than volume diffusion in the two minerals so that mass exchanges freely along grain boundaries among minerals within the REV (e.g., Eiler et al. 1992). Assumption (4) allows us to relate concentrations of a trace element at the surface of the two minerals through a mineral–mineral partition coefficient, k_{AB} (Eqs. 14a–14c). Expression for the temperature- and pressure-dependent diffusion coefficient for the

trace element of interest in mineral B is the same as that for mineral A, i.e., by replacing subscript A in Eq. (2) with subscript B.

An algebraic equation for the mean closure temperature in cooling bi-mineralic systems at a constant pressure was derived by comparing cooling time constant and diffusive re-equilibration time (Liang 2015). Following the procedure of Liang (2015) and that outlined in the section "Generalization", we obtain an algebraic expression for the mean closure temperature in cooling and upwelling bi-mineralic systems,

$$\frac{\phi_B H_A^{\text{u-p}} \frac{d_A^2 \dot{s}}{D_A^c} + \phi_A k_{AB}^c H_B^{\text{u-p}} \frac{d_B^2 \dot{s}}{D_B^c}}{\left(\phi_A k_{AB}^c + \phi_B\right) RT_c^{\,2}} + \frac{\phi_B \phi_A k_{AB}^c H_k^{\text{u-p}}}{\left(\phi_A k_{AB}^c + \phi_B\right)^2 RT_c^{\,2}} \left(\frac{d_A^2}{D_A^c} - \frac{d_B^2}{D_B^c}\right)\dot{s} = \exp(G), \tag{18}$$

where G is the geometry function of Dodson (1973). The path-dependent enthalpies for diffusion and mineral–mineral partitioning take on the general form

$$H_m^{\text{u-p}} = E_m + \left[P_{\text{ref}} - \left(\frac{\mathrm{d}P}{\mathrm{d}T}\right)_{\text{u-p}} T_{\text{ref}}\right] V_m, \quad m = A,\ B,\ \text{or}\ k. \tag{19}$$

The cooling rate $\dot{s}$, diffusion coefficients (D_A^c and D_B^c) and partition coefficient (k_{AB}^c) in Eq. (18) are evaluated at the closure temperature T_c and closure pressure P_c using expressions similar to Eq. (9c). As in mono-mineralic systems, the closure pressure is related to closure temperature through the upwelling path, i.e., Eq. (8c).

Appendix 2: Nonlinear upwelling paths

For diffusional loss along a nonlinear upwelling path, the pressure and temperature are also related to each other through the upwelling path in P–T space. We can make proper substitutions following methods similar to those outlined in this study. Here we consider two cases for cooling and upwelling mono-mineralic systems. Expressions for bi-mineralic systems can be easily obtained with reference to Eq. (18).

Case (a). $P = f(T)$. Replacing pressure by temperature in the Arrhenius equation, we have an equation for the mean closure temperature,

$$\frac{\left\{E_A + \left[f(T_c) - \left.\frac{\mathrm{d}f}{\mathrm{d}T}\right|_{T=T_c} T_c\right] V_A\right\}\dot{s}}{RT_c^2} \frac{d_A^2}{D_A^c} = \exp(G), \tag{20}$$

$$D_A^c = D_A^0 \exp\left[-\frac{E_A + f(T_c)V_A}{RT_c}\right], \tag{21}$$

where the slope of the upwelling path $\mathrm{d}P/\mathrm{d}T = \mathrm{d}f/\mathrm{d}T$ is evaluated at the closure temperature.

Case (b). $T = c_1 P + c_2 P^2$. This expression is related to steady-state heat conduction and geotherms of the lithosphere (e.g., Pollack and Chapman 1977) and was used in Yao (2015) in her study of the closure temperatures of REE in garnet–clinopyroxene aggregates. Here it is more convenient to calculate closure pressure (P_c) by considering the decompression rate. Replacing temperature by pressure in the Arrhenius equation, we have an equation for the mean closure pressure

$$\frac{\left[(E_A + P_c V_A)(c_1 + 2c_2 P_c) - (c_1 P_c + c_2 P_c^2)V_A\right]\dot{u}}{R(c_1 P + c_2 P_c^2)^2} \frac{d_A^2}{D_A^c} = \exp(G), \tag{22}$$

$$D_A^c = D_A^0 \exp\left[-\frac{E_A + P_c V_A}{R(c_1 P_c + c_2 P_c^2)}\right], \tag{23}$$

where $\dot{u} = \mathrm{d}P/\mathrm{d}t$ is the decompression rate and related to cooling rate through Eq. (5). The mean closure temperature is related to the mean closure pressure through the parabolic geotherm.

References

Albarède F (1995) Introduction to geochemical modeling. Cambridge University Press, Cambridge

Béjina F, Jaoul O, Liebermann RC (2003) Diffusion in minerals at high pressure: a review. Phys Earth Planet Interiors 139:3–20

Bjerg EA, Ntaflos T, Thöni M, Aliani P, Labudia CH (2009) Heterogeneous lithospheric mantle beneath northern Patagonia: evidence from Prahuaniyeu garnet- and spinelperidotites. J Petrol 50:1267–1298

Bloch E, Ganguly J, Hervig R, Cheng W (2015) ^{176}Lu–^{176}Hf geochronology of garnet I: experimental determination of diffusion kinetics of Lu^{3+} and Hf^{4+} in garnet, closure temperatures and geochronological implications. Contrib Miner Petrol 169:12

Brey G, Köhler T (1990) Geothermobarometry in four-phase lherzolites II. New thermobarometers, and practical assessment of existing thermobarometers. J Petrol 31:1353–1378

Carlson WD (2012) Rates and mechanism of Y, REE, and Cr diffusion in garnet. Am Miner 97:1598–1618

Chakraborty S (2010) Diffusion coefficients in olivine, wadsleyite and ringwoodite. Rev Miner Geochem 72:603–640

Chakraborty S, Ganguly J (1992) Cation diffusion in aluminosilicate garnets: experimental determination in spessartine-almandine diffusion couples, evaluation of effective binary diffusion coefficients, and applications. Contrib Miner Petrol 111:74–86

Cherniak DJ (2005) Yb and Y diffusion in grossular garnet. Geochim Cosmochim Acta 69(suppl.):405

Cherniak DJ, Watson EB (2007) Ti diffusion in zircon. Chem Geol 242:473–486

Cherniak DJ, Watson EB (2012) Diffusion of helium in olivine at 1 atm and 2.7 GPa. Geochim Cosmochim Acta 84:269–279

Chu X, Ague JJ (2015a) A new statistical analysis of rare earth element diffusion data in garnet. American Geophysical Union, Fall Meeting, abstract #V13A-3092

Chu X, Ague JJ (2015b) Analysis of experimental data on divalent cation diffusion kinetics in aluminosilicate garnets with application to timescale of peak Barrovian metamorphism, Scotland. Contrib Miner Petrol 170:25

Dodson MH (1973) Closure temperature in cooling geochronological and petrological systems. Contrib Miner Petrol 40:259–274

Dodson MH (1976) Kinetic processes and thermal history of slowly cooling solids. Nature 259:551–553

Dodson MH (1986) Closure profiles in cooling systems. Mat Sci Forum 7:145–154

Eiler JM, Baumgartner LP, Valley JW (1992) Intercrystalline stable isotope diffusion: a fast grain boundary model. Contrib Miner Petrol 112:543–557

Freer R, Edwards A (1999) An experimental study of Ca-(Fe,Mg) interdiffusion in silicate garnets. Contrib Miner Petrol 134:370–379

Ganguly J, Tirone M (1999) Diffusion closure temperature and age of a mineral with arbitrary extent of diffusion theoretical formulation and applications. Earth Planet Sci Lett 170:131–140

Ganguly J, Tirone M (2001) Relationship between cooling rate and cooling age of a mineral: theory and applications to meteorites. Meteorit Planet Sci 36:167–175

Gardés M, Montel J-M (2009) Opening and resetting temperatures in heating geochronological systems. Contrib Miner Petrol 158:185–195

Grasemann B, Ratschbacher L, Hacker BR (1998) Exhumation of ultrahigh-pressure rocks: thermal boundary conditions and cooling history. In: Hacker BR, Liou JG (eds) When continents collide: geodynamics and geochemistry of ultrahigh-pressure rocks. Kluwer Academic Publishers, Berlin, pp 117–139

Guillot S., Hattori K., Agard P., Schwartz S. and Vidal O. (2009) Exhumation processes in oceanic and continental subduction contexts: a review. In: Lallemand S, Funiciello F (eds) Subduction zone geodynamics. Springer, Berlin, pp 175–205

Holzapfel C, Chakraborty S, Rubie DC, Frost DJ (2007) Effect of pressure on Fe–Mg, Ni and Mn diffusion in $(Fe_xMg_{1-x})_2SiO_4$ olivine. Phys Earth Planet Interiors 162:186–198

Lasaga AC (1998) Kinetic theory in the earth sciences. Princeton University Press, Princeton

Liang Y (2014) Time scales of diffusive re-equilibration in bi-mineralic systems with and without a fluid phase. Geochim Cosmochim Acta 132:274–287

Liang Y (2015) Simple models for closure temperature of a trace element in cooling bi-mineralic systems. Geochim Cosmochim Acta 165:35–43

Müller T, Massonne H-J, Willner AP (2015) Timescales of exhumation and cooling inferred by kinetic modeling: an example using a lamellar garnet pyroxenite from the Variscan Granulitgebirge, Germany. Am Miner 100:747–759

Pollack HN, Chapman DS (1977) On the regional variation of heat flow, geotherms, and lithospheric thickness. Tectonphysics 38:279–296

Powell R, White L (1995) Diffusive equilibration between minerals during cooling: an analytical extension to Dodson's equation for closure in one dimension. Geol J 30:297–305

Scambelluri M, Pettke T, Van Roermund HLM (2008) Majoritic garnets monitor deep subduction fluid flow and mantle dynamics. Geology 36:59–62

Smart KA, Heaman LM, Chacko T, Simonetti A, Kopylova M, Mah D, Daniels D (2009) The origin of high-MgO diamond eclogites from the Jericho Kimberlite, Canada. Earth Planet Sci Lett 284:527–537

Sneeringer M, Hart SR, Shimizu N (1984) Strontium and samarium diffusion in diopside. Geochim Cosmochim Acta 48:1589–1608

Spengler D, van Roermund HLM, Drury MR, Ottolini L, Mason PR, Davies GR (2006) Deep origin and hot melting of an Archaean orogenic peridotite massif in Norway. Nature 440:913–917

Sun C, Liang Y (2014) An assessment of subsolidus re-equilibration on REE distribution among mantle minerals olivine, orthopyroxene, clinopyroxene, and garnet in peridotites. Chem Geol 372:80–91

Sun C, Liang Y (2015) A REE-in-garnet–clinopyroxene thermobarometer for eclogites, granulites and garnet peridotites. Chem Geol 393–394:79–92

Van Orman JA, Grove TL, Shimizu N (2001) Rare earth element diffusion in diopside: influence of temperature, pressure, and ionic radius, and an elastic model for diffusion in silicates. Contrib Miner Petrol 141:687–703

Van Orman JA, Grove TL, Shimizu N (2002a) Diffusion fractionation of trace elements during production and transport of melt in Earth's upper mantle. Earth Planet Sci Lett 198:93–112

Van Orman JA, Grove TL, Shimizu N, Layne GD (2002b) Rare earth element diffusion in a natural pyrope single crystal at 2.8 GPa. Contrib Mineral Petrol 142:416–424

Watson EB, Baxter EF (2007) Diffusion in solid-Earth systems. Earth Planet Sci Lett 253:307–327

Watson EB, Cherniak DJ (2013) Simple equations for diffusion in response to heating. Chem Geol 335:93–104

Yao L (2015) Closure temperature and closure pressure in bi-mineralic systems with applications to REE-in-two-mineral thermobarometers. Ph.D. Thesis, Brown University

Zhang Y (2008) Geochemical kinetics. Princeton University Press, Princeton